

Photo Catalytic Degradation Effect Of Green And Chemically Synthesized Bismuth Oxide Nanoparticles On Congo Red Dye

¹G.Jayapriya, ²T.Maheswari, ³M.Vennila

¹Research Scholar, ²Research Scholar, ³Assistant Professor

GOVERNMENT ARTS COLLEGE, DHARMAPURI, TAMILNADU, INDIA

Abstract - In the present study, we have reported the green and chemical synthesis and characterization of bismuth oxide nanoparticles using *Anisomeles malabarica* leaf extract as a natural surfactant. Degradation of Congo Red (CR) dye in aqueous solutions was investigated by means of photo catalysis of bismuth oxide which was synthesized by green and chemical methods. Efficiency of bismuth oxide for photo catalytic degradation under visible irradiation was studied by investigating the effects of amount of bismuth oxide, irradiation time, initial concentration and pH. It was found that complete decolorization is achieved within 30 min of irradiation. Results proved that bismuth oxide (green method) nanoparticles show more enhanced photo catalytic activity when compared to bismuth oxide (chemical method) nanoparticles. The prepared bismuth oxide nanoparticles have been characterized by UV-Vis absorption spectroscopy, X-ray diffraction (XRD), Fourier transform infrared spectroscopy (FT-IR), and scanning electron microscopy (SEM).

keywords - *Anisomeles malabarica*, bismuth oxide, congo red dye, dye degradation, isotherm.

Introduction

Nanomaterials (NMs) are defined as materials with at least dimension in the size range from approximately 1-100 nanometers. A focused integration of bio and nano techniques for biological synthesis of NMs, known as bio nanotechnology, has emerged from nanotechnology^[1-3]. The synthesis combines biological principles (i.e., reduction/oxidation) by microbial enzymes or plant phytochemicals with physical and chemical approaches to produce nano-sized particles. Nanoparticles (Nps) are solid particles with all three external dimensions at the nano scale^[4-10] that can drastically modify physico-chemical properties compared to the bulk material. It can explicate actions depending on the chemical composition, biological actions, size and shape^[11-13]. Bismuth is one of the most interesting materials which can transit from semi-metal to semiconductor when its crystallite is small enough Dechong Ma et.al^[14]. Recently, many reports have been published in the literature on the synthesis of bismuth NPs from bismuth ions using chemical and radiolytic reducing methods, electron irradiation and microwave treatment Kharissova et.al^[15]. Dyes are extensively used in the industrial sector such as the textile industry, rubber, paper, leather and cosmetics G. Alagumuthu et.al^[16]. However, the discharge of dyes could lead to water pollution problems because of their toxicity. Several techniques are used to remove such contaminants. The techniques can be categorized into conventional methods such as adsorption, coagulation, and flocculation; established methods such as ion exchange, membrane separation, and oxidation; and emerging methods such as biodegradation and microbial treatment N. Pandey et.al^[17]. Currently, the removal process based on photocatalysis is attracting great attention at the applied research level as a possible solution to the environmental pollution problem. The primary mechanism of this process involves the decomposition of organic contaminants into carbon dioxide and water by utilizing light energy. Semiconductor photocatalysts absorb the light energy, thus initiating the oxidation reactions by generating hole (h⁺) and electron (e⁻) pairs, which can generate free radicals such as hydroxyl (•OH) radicals N. Soltani et.al^[18]. These free radicals work as oxidizers of organic pollutants. Therefore, the photocatalytic oxidation reaction requires a source of light with energy in the visible or UV spectrum or solar energy. *Anisomeles malabarica* (L) is a traditional medicinal plant, distributed throughout India. It has been used in folk medicine for the treatment of cancer, liver disorder, stomach ailment, fever, cold and cough^[19-20]. In this study, we first report about green leaf synthesis of bismuth oxide Nps from *A. malabarica* which were characterized by UV Vis spectroscopy, XRD, FT-IR, SEM study and their photo catalytic activity was performed.

MATERIALS AND METHODS:

Bismuth nitrate pentahydrate (Bi(NO₃)₃•5H₂O) purchased from MERCK. Nitric acid (HNO₃, 70%) and citric acid purchased from Sigma-Aldrich. Ethanol and hexane purchased from MERCK. All the reagents were used without further purification.

2.1 Preparation of *Anisomeles malabarica* leaf Extract

Anisomeles malabarica leaves were collected, washed and rinsed thoroughly in double distilled water to remove the dust particles and shade dried in open air. Dried leaves were powdered using mortar and pestle. 10g of powdered sample is macerated with 100ml of hexane for 20 min, then filtered to remove heavy biomaterials. The dried sample is boiled with 100ml of double distilled water for 10 min cooled, filtered and stored in refrigerator for further analysis.

2.2.1 Biosynthesis of Bismuth oxide nanoparticles from leaf extract

Aqueous solution of 0.001N Bismuth Nitrate was prepared using double distilled water. 50ml of freshly prepared leaf extract was added to 50ml of Bismuth Nitrate and the p^H of the solution is maintained at pH 3. Green color changed to brown color and stirred the solution for two hours using magnetic stirrer and kept the solution at warm temperature for reduction of Bi ions to Bismuth oxide nanoparticles Hammer K A et.al^[21].

2.2.2 Chemical synthesis of Bismuth oxide nanoparticles

Bismuth nitrate and urea were used for the preparation of Bi_2O_3 are of AR grade. A known quantity of $Bi(NO_3)_3 \cdot 5H_2O$ was dissolved in nitric acid solution and mixed with citric acid in 1:5 molar ratio. The above solution was stirred for 2hrs, and then heated until the precipitate of Nano crystalline Bi_2O_3 is formed Muthukrishnan Suriyavathana^[22].

2.4 Characterization Techniques

2.4.1 UV-Vis spectra Analysis

The formation of Bismuth oxide nanoparticles were confirmed by measuring the wavelength of reaction mixture in the UV-Vis spectrum of the PerkinElmer spectrometer at a resolution of 1nm (from 300 to 600) in 2ml quartz cuvette with 1 cm path length.

2.4.2 SEM Analysis

The SEM analysis was carried out to identify the size and morphology of the nanoparticles using JEOL-JEM 5600 LV.

2.4.3 FT-IR

FT-IR measurements were carried out to identify the potential functional groups in the leaf extract of *Anisomeles malabarica* which are responsible for the reduction of the Bi ions into Bi nanoparticles using PERKIN ELMER-AXIS spectrometer in the reflectance mode at a resolution of $4cm^{-1}$.

2.4.4 XRD analysis

The X-ray diffraction (XRD) pattern of the sample was measured using an x-ray diffractometer (BDX3300) with a reference target, Cu $K\alpha$ radiation ($\lambda=0.154nm$) voltage, 30 kV, and current, 30 mA. The sample was measured from 10° to 70° with steps of $4^\circ/min$.

2.5 Dye degradation studies:

2.5.1 Preparation of stock solution

Stock dye solution of congo red dye was prepared by dissolving 0.1g of it in water and making it up to 100ml in standard flask.

2.5.2 Determination of maximum absorption for the congo red dye

The wavelength at which maximum absorbance of dye solution takes place was checked by scanning the absorbance of the dye at different wavelength using ELICO SL-159 UV-VIS spectrophotometer.

2.6 Degradation studies

2.6.1 Variation of dosage

Congo red dye solution (100ml, 5mg/l) with Bismuth oxide different doses (0.2-1g) in different pyrex bottles. The pyrex bottles were placed in a mechanical shaker and shaken for 30 min. The dye solution was then filtered in a filter paper and absorbance was measured.

2.6.2 Variation of dye concentration

Congo red dye solution (3,4,5,6,7,mg/l) with 20ml of water were taken in pyrex bottles containing 0.5g of dosage. The bottles were placed in mechanical shaker for 30min. Each dye solution was then filtered in a ordinary filter paper. The absorbance was measured.

2.6.3 Variation of pH

Congo red dye solution (5mg/l) with 20ml of water and 0.5g of dosage were taken in pyrex bottles containing pH (2,4,7,10,12). The pyrex bottles were placed in a mechanical shaker and shaken for 30min. The dye solution was then filtered in a ordinary filter paper and absorbance were measured.

2.6.4 Variation of time

Congo red dye solution with the concentration 5mg/l was prepared and taken in a pyrex bottle containing 0.5g of dosage and pH-10 was maintained. The bottle was then placed in a mechanical shaker at room temperature. The dye solution was then filtered and absorbance was measured at every 10min.

Freundlich isotherm

Freundlich isotherm of sorption of congo red dye at different concentration using the sorbent dosage of 0.4g and shown in (fig – 15, 22) (Table -1,3)

The freundlich adsorption isotherm was calculated using the following equation

$$\ln q_e = \ln K_f + 1/n \ln C_e$$

Where K_f and n indicates the adsorption capacity and adsorption intensity where the values are obtained by plotting $\ln q_e$ versus C_e .

Langmuir isotherm

(Fig-16,23) (Table- 2,4) shows the equilibrium data fitted with Langmuir isotherm for the adsorption of congo red at different initial concentrations with sorbent dosage of 0.4g

Langmuir adsorption can be defined as per the following equation

$$C_e/q_e = (1+bc_e)/Q_0b$$

Where q_e is the quantity of dye adsorbed per unit weight of sorbent at equilibrium. Q_0 is the maximum possible amount of dye that can be adsorbed per unit weight of sorbent to form a complete monolayer on the surface, b is the empirical constant, indicating the affinity of sorbent towards the sorbate. The plot C_e/q_e versus C_e found to be liner. Adsorption capacity $Q_0 = 0.3428$

and adsorption desorption energy constant $b=0.0291$. The isotherm can be expressed by an equilibrium parameter (R_i) $=1/(1+bc_i)$. The R_i value is found to be less than 1. Hence the process is a favorable, spontaneous process.

Results and discussion

FT-IR Spectrum:

The results were further reinforced by FT-IR analysis, which showed the shifts and difference in areas of the peaks. By means of this technique, it is possible to identify the biomolecules in plant extracts which play the crucial role in the processes of reduction and stabilization of bismuth nanoparticles by green synthesis methods M. Mallahi et.al^[24]. (Fig-1) is the IR spectrum of Bismuth oxide nanoparticle chemical synthesis. The peaks observed at 1365cm^{-1} , 1289cm^{-1} and 1034cm^{-1} are due to primary alcohol C-O stretching. The peaks 814cm^{-1} and 667cm^{-1} are due to C-H stretching. (Fig-2) is the IR spectrum of Bi nanoparticle green synthesis. The peaks observed at 1327cm^{-1} , 1288cm^{-1} and 1038cm^{-1} are due to primary alcohols C-O stretching. The peaks at 845cm^{-1} , 814cm^{-1} and 667cm^{-1} are due to substituted C-H stretching.

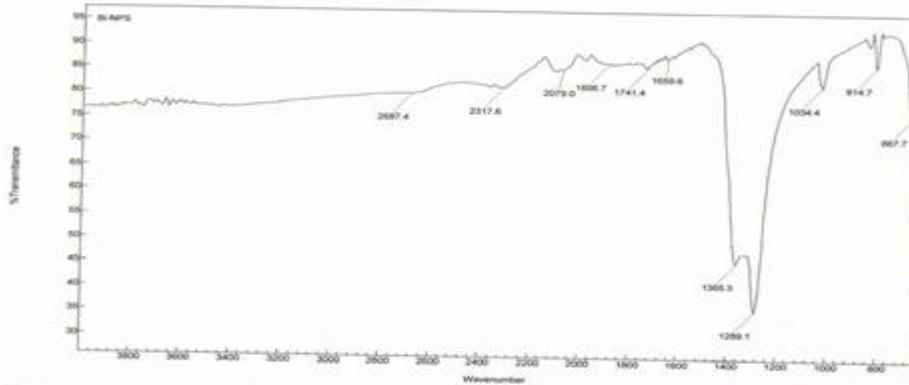


Fig-1 FT-IR Spectrum of Bismuth oxide nanoparticles (chemical synthesis)

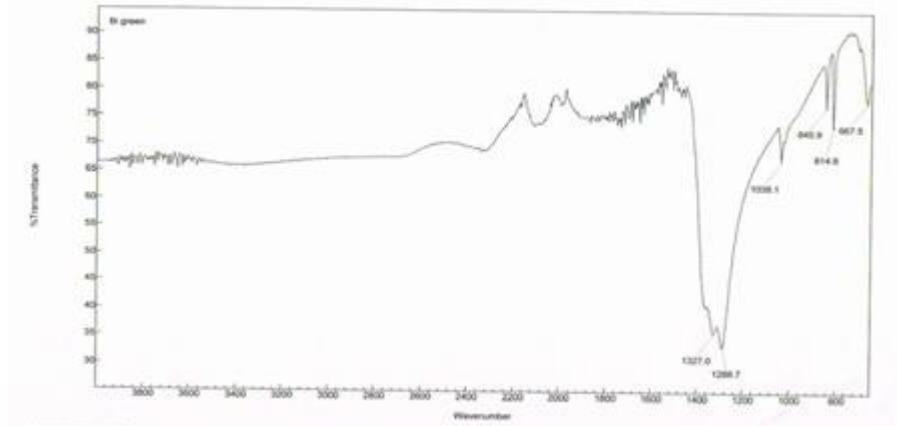


Fig-2 FT-IR spectrum of biosynthesis of Bismuth oxide nanoparticles in *Anisomeles malabarica*

UV-Visible spectroscopy

Wavelength at which at maximum absorbance takes place by the synthesized nano particles was calculated by measuring the absorbance of the solution at various wave length. The maximum absorbance was found to be in the range of 319nm (Fig-3) which also confirms the formation of Bismuth oxide nanoparticles by green synthesis maximum absorbance at 318nm (fig-4) which also confirms the formation of bismuth oxide nanoparticles by chemical synthesis.

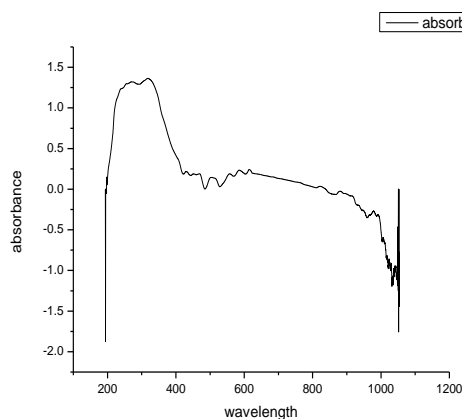


Fig-3 Green synthesis Bi_2O_3 Nps

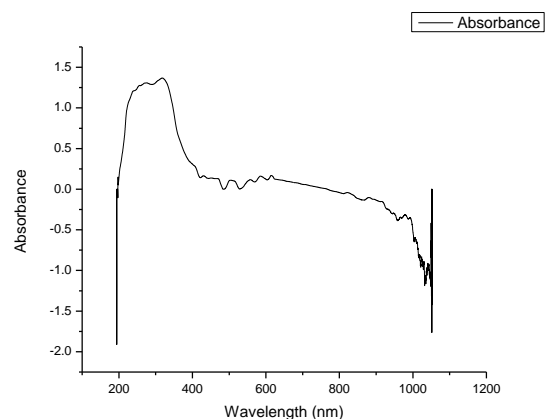
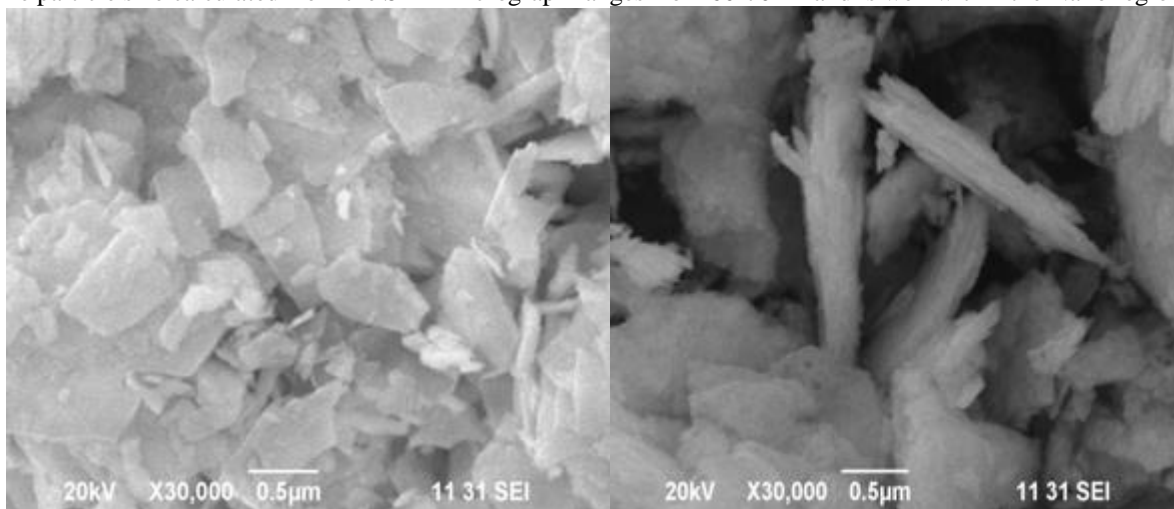


Fig-4 Chemical synthesis of Bi_2O_3 Nps

Scanning electron microscopy

SEM images of the obtained bismuth oxide nanoparticles. The synthesized bismuth oxide nanoparticles are agglomerated with a particle size ranging from below 100–190 nm. SEM image (Fig-5) shows the size and shape of the biosynthesized Bismuth oxide Nps using *Anisomeles malabarica* leaf extract. Spherical and rod shape of nanoparticles with highly agglomeration was noted with range from 50-100nm. (Fig-6) shows typical SEM image of chemically synthesized Bi oxide Nps grown in this study. The particle size calculated from the SEM micrograph ranges from 60-70nm and is well within the Nano region.

Fig:5 Green synthesis Bi₂O₃ nanoparticlesFig:6 chemical synthesis Bi₂O₃ nanoparticles

X-ray diffraction analysis

The XRD pattern of the synthesized bismuth oxide nanoparticles is shown in (Fig-7,8). The crystalline structure of synthesized bismuth oxide nanoparticles exhibited a hexagonal structure of the wurtzite (JCPDS no. 36-1451). The biosynthesized bismuth oxide nanoparticles 2θ values correspondence to (288),(282),(272),(270).(268) and based to chemically synthesized bismuth 2θ values are (216),(206),(200),(194),(192) [24].The average crystalline size of the both synthesized bismuth oxide were determined using Debye–Scherrer'. The crystalline size analysis investigated from the highly intense and sharp diffraction peak corresponds to the (288) diffraction by the following equation:

$$(D)= 0.9\lambda/\beta \cos \theta$$

where D is the average crystalline size, λ the CuK α radiation wavelength, i.e., 1.5414 Å, β the full-width at halfmaximum in radians and θ the scattering angle in degree. The average crystalline size of the synthesized bismuth oxide is 51.23 nm.

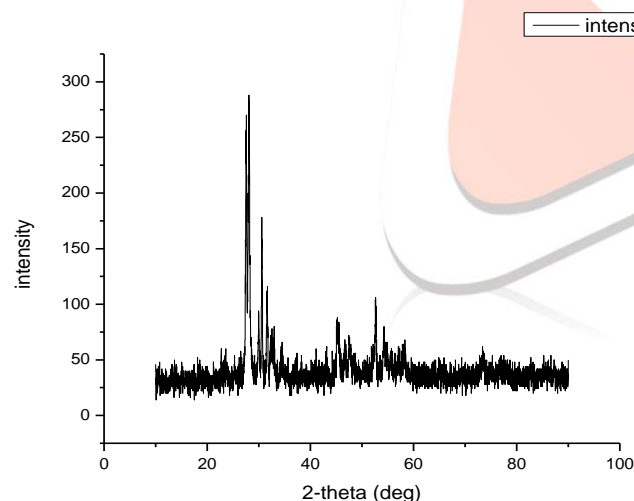


Fig-7 Green synthesis of bismuth oxide nanoparticle

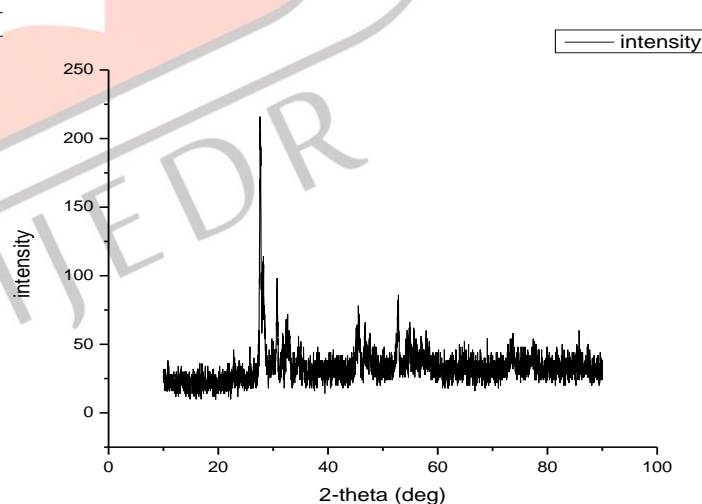


Fig-8 Chemical synthesis of bismuth oxide nanoparticles

3.2 Degradation Studies

3.2.1 Determination of λ_{\max} Congo red Dye Solution

The wavelength at which maximum absorbance of dye solution was found to be 490nm using UV-Vis spectrophotometer shown in(Fig -9).

3.2.2 Dye degradation studies using Bismuth oxide (Green synthesis)

Variation of dosage

Congo red dye solution (100ml, 5mg/l) is added with different doses of bismuth oxide nanoparticles (0.2-1g) and shaken for 30 min. 0.4g of Bismuth oxide was fixed as optimum dosage for removal of dye (Fig-10).

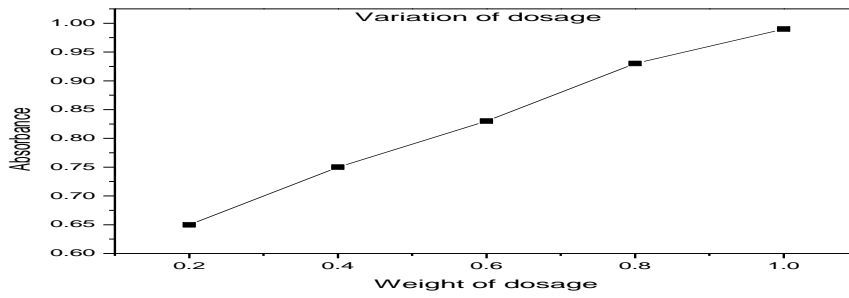


Fig-10

Variation of dye concentration

Congo red dye solution (3,4,5,6,7 mg/l) with 20ml of water were shaken with 0.4g of dosage. Percentage adsorption increases linearly with increases of initial dye concentration (Fig-11).

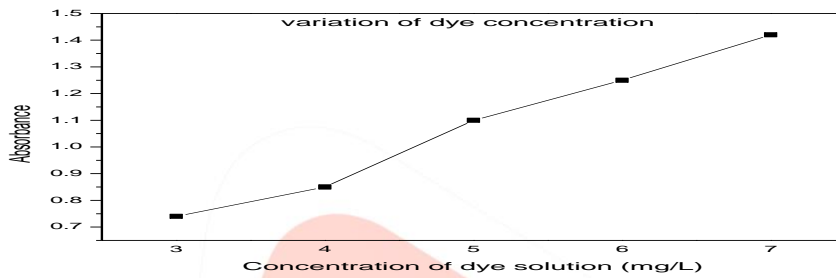


Fig -11

Variation of pH

Congo red dye solution (5mg/l) with 20ml of water and 0.4g of dosage were shaken in pyrex bottles containing solutions of pH (2,4,7,10,12). Percentage adsorption decreases linearly with increases of pH (Fig-12).

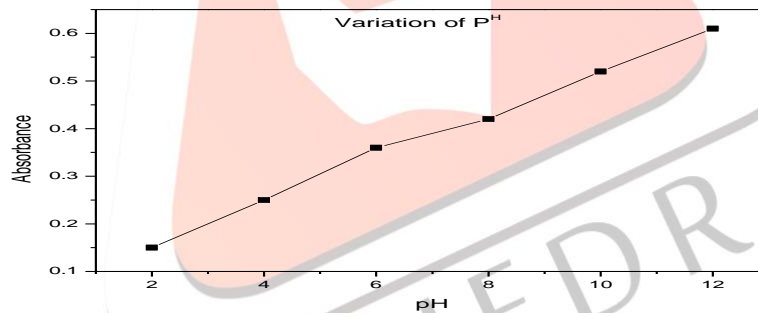


Fig-12

Variation of time

Congo red dye solution with the concentration 5mg/l was prepared and shaken with 0.4g of dosage at pH-8. Percentage adsorption reached equilibrium at 10 min shown in (Fig-13).

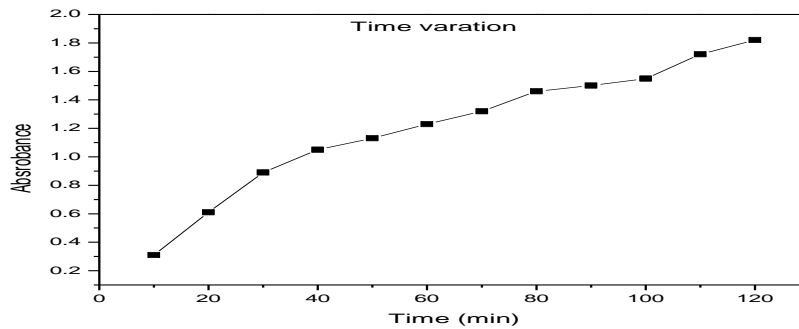


Fig-13

Calibration Details for Bismuth oxide (Green synthesis)

Hence the optimum conditions for the degradation of dye using the bismuth oxide nanoparticles was fixed as λ_{max} -490 nm, dosage-0.4g(2,4,6,8,10,mg/l), pH -8 and shaking time 40 min which is shown in (Fig-14).

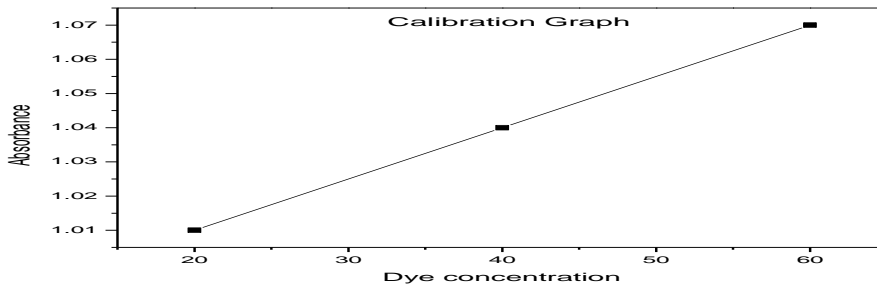


Fig-14

FREUNDLICH ISOTHERM (CONGO RED DYE)

TIME(min)	O.D	Ci (mg/l)	Ce (mg/l)	Qe (mg/g)	Lnqe	Ln Ce	3+lnqe
10	0.62	5	3.5	1.5	0.4054	1.2527	3.4054
20	0.59	5	2.4	2.6	0.9555	0.8754	3.9555
30	0.46	5	2.6	2.4	0.8754	0.9555	3.8754
40	0.37	5	2.1	2.9	1.0647	0.7419	4.0647
50	0.29	5	1.5	3.5	1.2522	0.4054	4.252
60	0.24	5	1.4	3.6	1.2809	0.3364	4.2809
70	0.28	5	1.2	3.8	1.3350	0.1823	4.3350
80	0.14	5	0.9	4.1	1.4109	-0.1053	4.4109
90	0.08	5	0.5	4.5	1.5040	-0.6931	4.5040
100	0.03	5	0.3	4.7	1.5475	-1.203	4.4575

Table -1

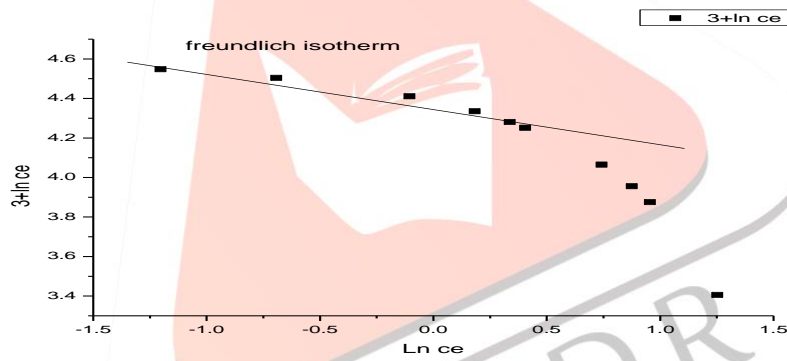


Fig-15

LANGMUIR ISOTHERM (CONGO RED DYE)

Time(min)	O.D	Ci(mg/l)	Ce(mg/L)	Qe(mg/g)	Ce/qe
10	0.62	5	3.5	1.5	2.33
20	0.59	5	2.4	2.6	0.92
30	0.46	5	2.6	2.4	1.08
40	0.37	5	2.1	2.9	0.72
50	0.29	5	1.5	3.5	0.42
60	0.24	5	1.4	3.6	0.41
70	0.28	5	1.2	3.8	0.31
80	0.14	5	0.9	4.1	0.21
90	0.08	5	0.5	4.5	0.11
100	0.03	5	0.3	4.7	0.06

Table -2

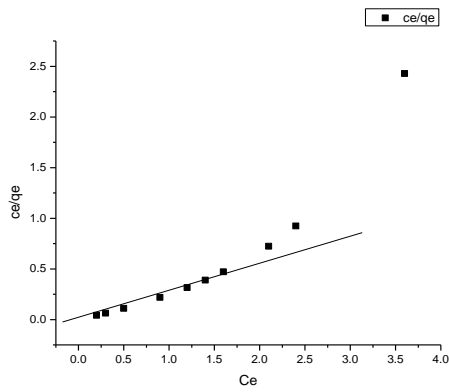


Fig-16

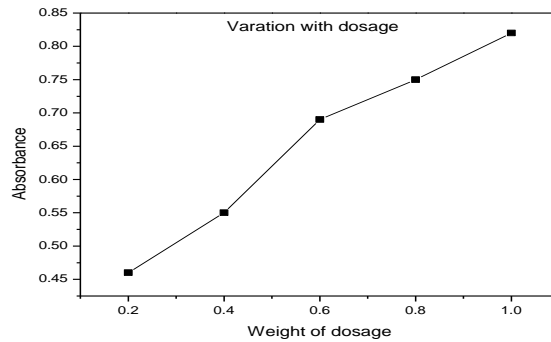


Fig-17

3.2.3 Dye degradation studies using bismuth oxide nanoparticles (chemical synthesis)

The similar procedure was followed for the characterization of bismuth oxide nanoparticles prepared by sol-gel method to fix the dosage (Fig-17), concentration (Fig-18), pH (Fig-19) and shaking time (Fig-20).

Variation of dosage

Variation of dye Concentration

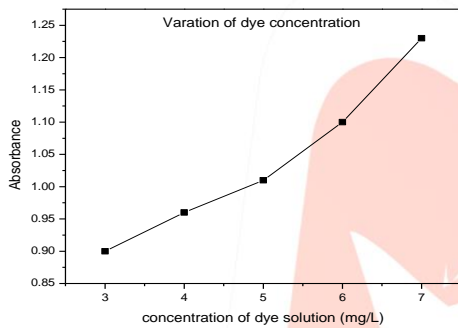


Fig-18

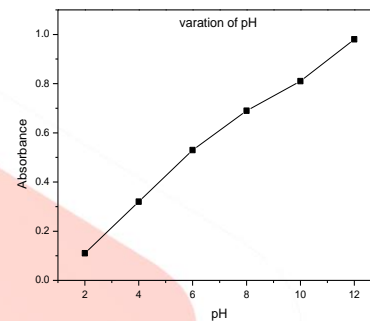


Fig-19

Variation of Time

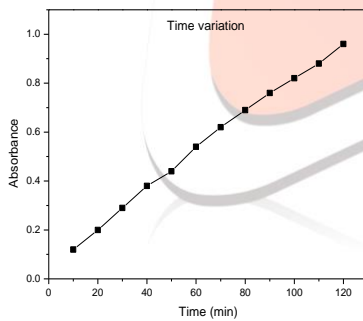


Fig-20

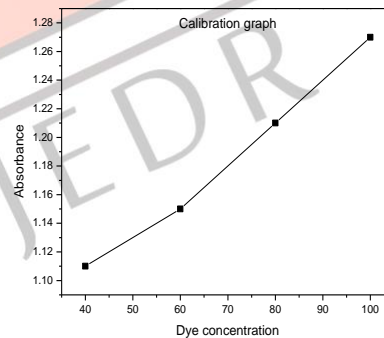


Fig-21

Calibration graph for Bismuth oxide nanoparticles (Chemical Synthesis)

FREUNDLICH ISOTHERM

Time(min)	O.D	Ci(mg/l)	Ce(mg/l)	Qe(mg/l)	Ln Ce	Lnqe	3+LnCe
10	0.65	5	3.6	1.4	0.3364	1.280	3.3364
20	0.43	5	2.4	2.6	0.9555	0.875	3.9555
30	0.39	5	2.9	2.9	1.0647	0.741	4.0647
40	0.31	5	3.4	3.4	1.2237	0.470	4.2237
50	0.28	5	3.6	3.6	1.2809	0.336	4.2809
60	0.24	5	3.8	3.8	1.3350	0.182	4.3350
70	0.18	5	4.1	4.1	1.4109	-0.1053	4.4119
80	0.13	5	4.5	4.5	1.5050	-0.693	4.5040
90	0.08	5	4.7	4.7	1.5475	-1.203	4.5879
100	0.06	5	4.8	4.8	1.5683	-1.609	4.5468

Table-3

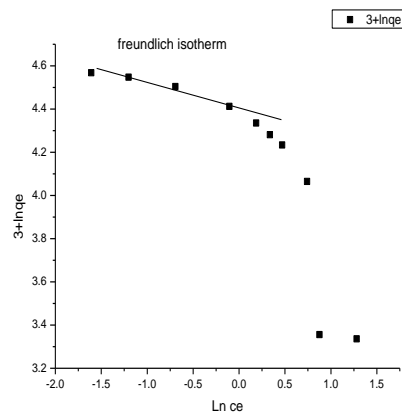


Fig-22

LANGMUIR ISOTHERM

Time(min)	O.D	Ci(mg/l)	Ce(mg/l)	Qe(mg/l)	Ce/qe
10	0.65	5	3.6	1.4	2.4285
20	0.43	5	2.4	2.6	0.9230
30	0.39	5	2.1	2.9	0.7241
40	0.31	5	1.6	3.4	0.4705
50	0.28	5	1.4	3.6	0.3888
60	0.24	5	1.2	3.8	0.3157
70	0.18	5	0.9	4.1	0.2195
80	0.13	5	0.5	4.5	0.1111
90	0.08	5	0.3	4.7	0.0638
100	0.06	5	0.2	4.8	0.0416

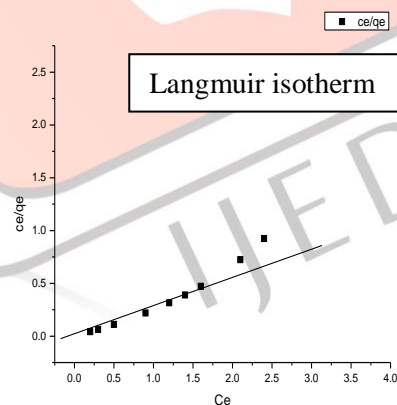


Fig-23

Conclusion

Green nanotechnology is gaining importance due to the elimination of harmful reagents and provides effective synthesis of expected products in an economical manner. Green synthesis of Bismuth oxide nanoparticle shows more compatible, eco-friendly, low cost and less time consuming process. Here, the Bismuth nanoparticle chemically and green synthesized using plant leaf extract of *Anisomeles malabarica* and characterized by UV-VIS spectrophotometer, FT-IR spectroscopy, Scanning electron microscopy and x-ray diffractometer. The biodegradation of congo red dye was studied using Bismuth oxide nanoparticles synthesized by both chemical and green route. The results obtained from degradation studies and isotherm studies proved that the degradation of dye was very effective using biosynthesized bismuth oxide nanoparticles compared to the chemically synthesized Bismuth oxide nanoparticles.

References

- [1] D.K. Sobha, K. Surendranath, V. Meena, K.T. Jwala, N. Swetha and K.S.M. Latha, Emerging trends in nanobiotechnology, *J. Biotech. Mol. Bio. Rev.*, **5(1)**, 001-012, 2010.
- [2] K. Sahayaraj and S. Rajesh, Bionanoparticles synthesis and antimicrobial applications, *Science against microbial pathogens: communicating current research and technological advances*, 228-244, 2011.

- [3] N. Krithiga, A. Jayachitra and Rajalakshmi, Synthesis, characterization and analysis of the effect of copper oxide nanoparticles in biological systems, *An Indian Journal of NanoScience*, **1(1)**,6-15, 2013.
- [4] P. Ball, Natural strategies for the molecular engineer, *Nanotechnology*, **13**, 15-28, 2002.
- [5] M.C. Roco, Broader societal issue of nanotechnology, *Journal of Nanoparticle Research*, **5**, 181-189, 2003.
- [6] Absar Ahmad, Priyabrata Mukherjee, Satyajyoti Senapati, Deendayal Mandal, M. Islam Khan, Rajiv Kumar and Murali Sastry, Extracellular biosynthesis of silver nanoparticles using the fungus *Fusarium oxysporum*, *Colloids Surf., B*, **28(4)**, 313-318, 2003.
- [7] V.J. Mohanraj and Y. Chen, —Nanoparticles – —A Review, *Tropical Journal of Pharmaceutical Research*, **5(1)**, 561-573, 2006.
- [8] P. Mohanpuria, N.K. Rana and S.K. Yadav, Biosynthesis of nanoparticles: Technological concepts and future application, *J. Nanoparticle Res.*, **7**, 9275-9280, 2007.
- [9] Ruffini Castiglione Monica and Roberto Cremonini, Nanoparticles and higher plants, *Caryologia*, 161-165, 2009.
- [10] M. Badanavalu, Prabhu, F. Syed Ali, C. Richard. Murdock, Saber M. Hussain and Malathi Srivatsan, Copper nanoparticles exert size and concentration dependent toxicity on somato sensory neurons of rat, *Nanotoxicology*, 150–160, 2010.
- [11] A. Nel, T. Xia, L. Madler and N. Li, Toxic potential of materials at the nanolevel, *Science*, 622-627, 2006.
- [12] T.I. Brunner, P. Wick, P. Manser, P. Spohn, R.N. Grass, L.K. Limbach, A. Bruinink and W. J. Stark, In vitro cytotoxicity of oxide nanoparticles: comparison to asbestos, silica, and effect of particle solubility, *Environmental Science & Technology*, **40**, 4374-4381, 2006.
- [13] Elena Masarovičová and Katarína Kráľová, Metal Nanoparticles and Plants, *Ecol Chem Engs*, **20(1)**, 9-22, 2013.
- [14] Dechong Ma, Jingzhe Zhao, Yan Zhaoa, Xinli Haoa, Linzhi Li, Li Zhang, Yan Lu, Chengzhong Yu, Synthesis of bismuth nanoparticles and self-assembled nanobelts by a simpleaqueous route in basic solution, *Physicochemical and Engineering Aspects*, **395**, 276-283, (2012).
- [15] Kharissova, O.V., Kharisov, B.I.: ‘Nanostructured forms of bismuth’, *Synth. React.Inorg. Met.-Org. Nano-Met. Chem.* **38**, 491–502, 2008.
- [16] G. Alagumuthu and T. Anantha kumar, “Structural, optical and photocatalytic activity of polymer capped zinc selenide nanoparticles,” *International Research Journal of Engineering and Technology*, **vol. 3,(11)**, 1022–1028, 2016.
- [17] N. Pandey, S. K. Shukla, and N. B. Singh, “Water purification by polymer nanocomposites: an overview,” *Nanocomposites*, **vol. 3(2)**, 47–66, 2017.
- [18] N. Soltani, S. Elias, M. Z. Hussein et al., “Visible light-induced degradation of methylene blue in the presence of photocatalytic ZnS and CdS nanoparticles,” *International Journal of Molecular Science*, **vol. 13(12)**, 12242–12258, 2012.
- [20]. Vijayalakshmi R, Ranganathan R. Chemopreventive effect of *Anisomeles Malabarica* whole plant extracts during DMBA induced hamster buccal pouch carcinogenesis, *Asian Journal of Pharmaceutical and Clinical Research*, **5(3)**, 185-188, 2012.
- [21] Hammer K A, Carson C F, Riley T V. Antimicrobial activity of essential oils and other plant extracts, *J App microbial*, **86(6)**, 985-900, 1999.
- [22]. Muthukrishnan Suriyavathana, *IJPRBS*, **Vol 4(5)**, 232-241, 2015.
- [23]. M. Mallahi¹, A. Shokuhfar², M. R. Vaezi³, A. Esmaeilirad⁴, V. Mazinan, Synthesis and characterization of Bismuth oxide nanoparticles via sol-gel method” *American Journal of Engineering Research (AJER)* **Vol-03(04)**, 162-165, 2014.
- [24]. Wang H, Li C, Zhao H, Li R and Liu J *Powder Technol.* 239- 266, 2013.